1.55 µm hybrid waveguide laser made by ion-exchange and wafer bonding

Marco Casale, Davide Bucci, Lionel Bastard, Jean-Emmanuel Broquin

▶ **To cite this version:**

PROCEEDINGS OF SPIE

1.55 μm hybrid waveguide laser made by ion-exchange and wafer bonding

Marco Casale, Davide Bucci, Lionel Bastard, Jean-Emmanuel Broquin

SPIE.

1.55 μm hybrid waveguide laser made by ion-exchange and wafer bonding

Marco Casale[*], Davide Bucci, Lionel Bastard and Jean-Emmanuel Broquin

Institut de Microélectronique, Electromagnétisme et Photonique-Laboratoire d'Hyperfréquence et Caractérisation, INP Grenoble – Minatec, 3 parvis Louis Néel, 38016 Grenoble Cedex 1, France

ABSTRACT

Distributed Feed Back (DFB) lasers working in the third telecom window are essential for optical communications, eye-safe sensors and lab-on-chip devices. Glass integrated optics technology allows realizing such devices by using rare-earth doped substrates. Despite their good output power and spectral characteristic, DFB lasers still present some reliability issues concerning the Bragg grating protection. Moreover Erbium doped glasses are not compatible with the realization of passive optical functions. In order to solve the DFB lasers reliability issues and to ensure a monolithic integration between active and passive functions, we propose an hybrid-device architecture based on ion-exchange technology and wafer bonding. The Ag^+/Na^+ ion-exchange in the silicate glass wafer is used to realize the passive functions and the lateral confinement of the electromagnetic field. Through a second ion exchange step, a slab waveguide is made on the Erbium-Ytterbium doped glass wafer. The Bragg grating is processed on the passive substrate and the two glasses are bonded. The potential of this structure has been demonstrated through the realization of a DFB hybrid laser with a fully encapsulated Bragg grating.

Keywords: ion-exchange, wafer bonding, hybrid structure, DFB laser, amplifier, glass integrated optics

1. INTRODUCTION

Distributed Feed Back (DFB) lasers realized by ion-exchange[1,2] on Er^{3+}/Yr^{3+} doped glass substrates are single mode sources with a narrow linewidth and stable emission in the third telecom window[3]. These characteristics, added to their compactness and their mW-range output power, make them convenient sources to be used in optical telecommunication systems[3] as well as in eye-safe detection system, such as LIDAR[4]. Usually, the architecture of such DFB lasers consists of an ion-exchanged waveguide and a Bragg grating etched on the glass surface, which provides the laser feedback. The grating patterned on the glass surface is actually one of the main remaining problems concerning the laser long-term reliability since it is fragile. This issue can be solved by encapsulating the Bragg grating with a passive glass by molecular bonding[5]. This technique presents the advantaged of not using any glue and being compatible with ion-exchange. A step further would be to use the passive glass to implement passive functions: e.g. a pump/signal duplexer. In this paper, we demonstrate the possibility of obtaining a DFB hybrid laser source on a passive substrate using the molecular bonding approach, opening the way to further active/passive functions integration[6]. Including the introduction this paper is divided in six sections. Section 2 presents the choice of an hybrid structure architecture, section 3 details the device fabrication process flow. In sections 4 and 5, the hybrid amplifier and the hybrid DFB laser are characterized. The conclusion is detailed in section 6.

2. HYBRID DEVICES ON GLASS SUBSTRATE

There are two different ways of integrating active functions on a passive ion-exchanged substrate using the glass bonding technique. The main difference between these two approaches is the way in which the guided electromagnetic field interacts with the active superstrate.

Evanescent field interaction with the active superstrate has been exploited in the device realized by Ohtsuhy et al.[7], shown in Fig.1-a). This device is fabricated by bonding an active Nd^{3+} doped fluoride glass on a passive Ag^+/Na^+ ion-

---

[*] Send correspondence to Marco Casale: E-mail : marco.casale@minactec.grenoble-inp.fr. Tel: +33 (0)4 5652 9484

exchanged silicate glass. The glasses refractive index and the ion-exchange parameters allowed obtaining evanescent interaction between the guided field and the superstrate. When pumped at 780 nm, a gain coefficient of 0.45 dB/cm has been reported for a signal wavelength of 1064 nm. However, because of the weak interaction between the guided light and the active substrate, the maximum gain coefficient attainable in this device is limited.

A second possibility is the structure shown in Fig. 1-b) realized by Gardillou et al[8]. In this case, a Tl^+/K^+ ion-exchanged passive silicate substrate is molecularly bonded with a high refractive index Er^{3+}/Yb^{3+} doped superstrate. The ion exchange and the thinning of the superstrate are tailored to obtain a strong field interaction with the active glass. In this structure the electromagnetic field is vertically confined by the active substrate and laterally confined by the ion-exchanged strip. The control of the active glass thickness is crucial to obtain a guiding structure: indeed, while a too thick slab would lead to a leaky structure, a thin slab would not guide the field. Thanks to a strong interaction of the guided field with the active glass, a gain coefficient of 3.66 dB/cm was measured for a signal wavelength of 1534 nm and a pump wavelength of 977 nm. Though, this structure presents a gain coefficient that is comparable with the one of state-of-the-art ion-exchanged amplifiers, the realization process involving lapping and polishing steps remains complex.

The Fig. 1-c) details the hybrid laser structure that we propose in this paper. The idea is to obtain a strong interaction between the guided field and the active superstrate, while avoiding the lapping and polishing processes. For this reason, a strip IE passive substrate is bonded with a slab IE active superstrate. The result is a dielectric structure in which the strip confines the field in the horizontal direction while the planar waveguide ensures the vertical confinement. The Bragg grating, providing the feedback, is patterned on the passive glass surface to realize the DFB Hybrid laser structure. Using this architecture the grating is encapsulated and protected thanks to the wafer bonding. Moreover choosing the most adapted glass substrates, this structure allows several possibilities for designing efficient active devices. Indeed, varying the different ion-exchanges parameters can make the behavior of the structure shift from an active slab waveguide one to a passive channel one presenting an evanescent interaction with the active slab. Therefore, this hybrid structure has the potential to gather all the qualities of a classical ion-exchanged DFB laser with a better reliability and life-time because of the grating encapsulation.
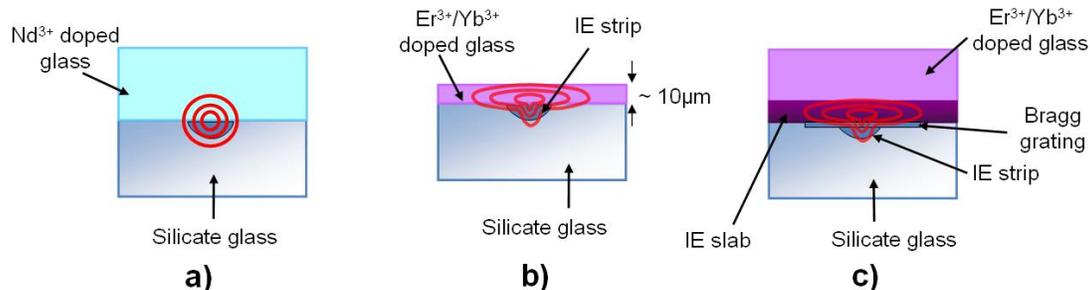

Figure 1: (a) evanescent interaction based amplifier (b) superstrate thinning based amplifier architecture (c) proposed hybrid DFB laser architecture

3. HYBRID STRUCTURE REALIZATION PROCESS

The two glass wafers chosen for the hybrid DFB laser are an ion exchange-dedicated silicate glass from Teem Photonics (GO14) for the passive one and a Schott IOG-1 Er^{3+}/Yb^{3+} codoped phosphate glass[9] for the active one. The IOG-1 doping concentrations are 2.2 wt% for Er_2O_3 and 3.6 wt% for Yb_2O_3, respectively. The maximum Er^{3+} emission cross-section is located at 1534 nm and the maximum Yb^{3+} absorption cross-section is at 980 nm.

3.1 Passive ion-exchange strip realization process

In order to realize the ion-exchanged confinement strip a 40nm-thick Al_2O_3 masking film is deposited on the glass surface by RF sputtering, Fig 2-b).With a standard photolithographic process, series of 4.5 cm-long straight diffusion apertures, whose width is ranging from $w = 0.5$ μm to $w = 10$ μm by step of 0.5 μm, are then defined, Fig 2-c). The ion-exchange will take place through these apertures when the substrate is immersed in a bath of molten $AgNO_3/NaNO_3$ salts Fig 2-d). The duration of the ion exchange t_{ex}, its temperature T, as well as the silver atoms molar concentration c_{Ag}, are the technological parameters that can be fixed by design. Once the ion exchange is finished, the alumina mask is

removed Fig 2-e). For the realization of an Optical Amplifier, the passive glass process can be considered as finished at this point, while for a DFB laser source an extra process step for the Bragg grating implementation must be carried-out.
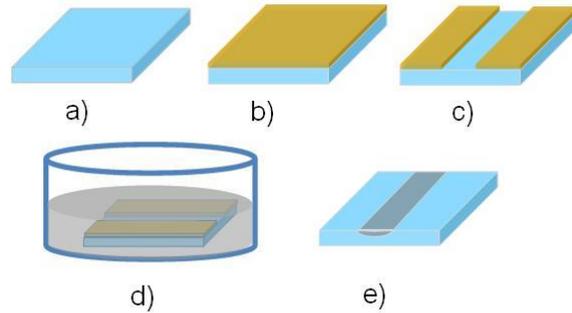

Figure 2: (a) passive glass wafer. (b) Al$_2$O$_3$ film deposition. (c) Al$_2$O$_3$ etching. (d) ion-exchange. (e) IE stripe.

Though the Bragg grating could be realized on either the passive or the active wafer, the silicate glass being less fragile, it has been decided to directly pattern the Bragg grating on its surface. The laser emission wavelength depends on the Er^{3+} emission spectrum and is defined by the grating period Λ_{Bragg} according to the Bragg law (1)

$$\lambda_B = 2\Lambda_{Bragg} n_{eff} \qquad (1)$$

where λ_B is the laser emission wavelength and n_{eff} is the effective index of the guided mode. Choosing the emission wavelength λ_B=1534 nm (which corresponds to the maximum of the Er^{3+} atom emission cross section in the IOG-1 glass) and knowing the effective index n_{eff} of the guided mode at this wavelength, we set Λ_{Bragg} to satisfy the Bragg condition. According to the structure design n_{eff} can vary between 1.513 and 1.590; we need a flexible technique to realize Λ_{Bragg} going from 482 nm to 507 nm, allowing a critical dimension of 247 nm and 253.5 nm respectively. For this reason, a holographic lithographic process has been chosen. After the lithography, the Bragg grating is transferred on glass using a RIE process based on SF$_6$ and CFH$_4$ gases. This etching procedure allows obtaining a grating depth ranging from 10 nm to 200 nm.

3.2 Active glass substrate processing and bonding

The technological process involving the IOG1 glass is quite straightforward: no lithography is needed as a slab waveguide has to be realized on the glass surface. The substrate is thus put in a bath of molten AgNO$_3$/NaNO$_3$ salts during a defined exchange time t_{ex}. The two ion-exchanged wafers are thoroughly cleaned in order to allow the creation of molecular bonds between then entailing the completion of the hybrid structure realization process.

4. HYBRID OPTICAL AMPLIFIER

During the bonding procedure, the Ag$^+$ ions can eventually reduce to metallic silver aggregates, which are sources of propagation losses. Thus, it is necessary, before realizing the hybrid DFB laser, to qualify the guiding properties of the hybrid structure realized with the process described above. For this reason an hybrid amplifier has been fabricated using the ion-exchange parameters summarized in Table 1.

Table 1.Summary of exchange parameters used to realize the hybrid amplifier.

	GO14	IOG-1
T	330°C	320°C
t_{ex}	3 min	3 min
c_{Ag}	1%	20%

4.1 Near field characterization

We first performed a mode profile characterization using a HI1060 FLEX fiber for the injection and imaging the mode intensity distribution through a microscope objective on a InGaAs CCD camera. We used two lasers sources emitting at wavelengths of 1550 nm and 1054 nm to study the number of propagation modes supported by the structure as well as their intensity distribution. The λ=1054 nm is chosen, being reasonably close to the pump wavelength $\lambda_p = 976.2$ nm, while avoiding absorption and emission of Er^{3+}, that could blur the image. The $\lambda = 1550$ nm measurement are simply affected by the Er^{3+} absorption, but the mode profile is not reshaped by the fluorescence. The hybrid structure is single mode at 1054 nm and 1550 nm for mask aperture width ranging between 1 μm to 6 μm.

The intensity shape of the guided modes can be seen in Fig. 2. The large mode profile is typical of hybrid structure where the ion exchanged strip mainly assures the lateral confinement and its influence is almost negligible concerning the vertical one.
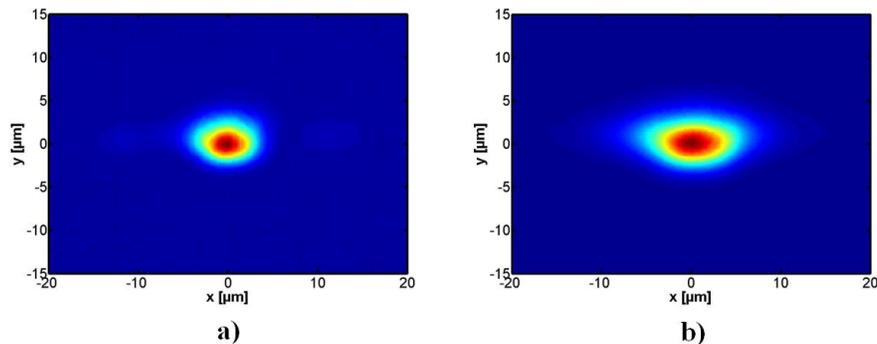

Figure 3: Near field mode profiles for an aperture $w = 6$ μm using a (a) $\lambda = 1054$ nm source and a (b) $\lambda = 1550$ nm one.

4.2 Insertion losses and gain characterization

The losses are measured for the waveguides presenting single mode operation at the pump and signal wavelengths. The measurement is done using a 1310 nm wavelength laser source since Er^{3+} and Yb^{3+} atoms do not absorb at this wavelength. The measurement setup is schematized in Fig. 4). A HI1060 FLEX fiber is used to inject the signal and a second one is adopted to bring the transmitted signal to the optical power-meter. We repeated the insertion losses measurement on waveguides of different length L (4.2 cm and 1.5 cm). For $w = 6$ μm waveguide we obtained (1.5±0.3) dB of coupling losses per facet and (0.3±0.3) dB/cm of propagation losses. The losses at the signal and pump wavelengths are expected to be of the same order of magnitude. The low propagation losses are compatible with the realization of an amplifying structure and exclude a high concentration of silver aggregates.
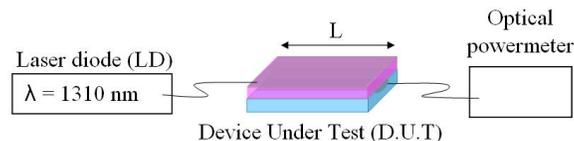

Figure 4: losses measurement optical setup

Fig. 5-a) presents the optical setup used to measure the device gain. A TUNICS tunable laser source, generating a wavelength λ=1534 nm, is connected through a SMF28 fiber to an optical attenuator needed to perform a small signal analysis. A second SMF28 fiber connects the optical attenuator to the 980 nm/1550 nm multiplexer. The λ_p laser diode source is connected the 980 nm branch of the multiplexer. The multiplexer output fiber (HI1060 Flex) is used to inject the two wavelengths into the 6 μm-wide waveguide under test. The $\lambda = 1534$ nm at the output of the device is measured with a calibrated optical spectrum analyzer (OSA) through an HI1060 Flex fiber.

With a launched pump power of 339.9 mW a (0.0±0.9) dB net gain has been obtained for a 1.6 cm-long waveguide, see Fig. 5-b). Subtracting the coupling losses, we obtain an actual gain of (3.0±0.9) dB and a gain coefficient of (1.9±0.9) dB/cm for this kind of device. Looking at the actual gain axis, we can see that the device becomes optically transparent for a launched pump power of 100 mW.
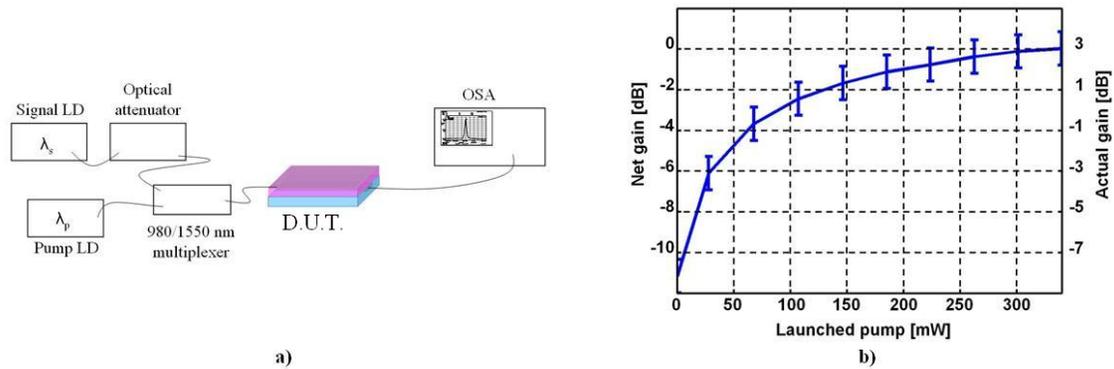
Figure 5: (a) Gain measurement optical setup. (b) Gain measurement within the 1.5 cm long waveguide at λ=1534 nm as a function of the pump launched power.

4.3 Fabry-Perot laser

With the measured gain of 3dB, by adding an optical feedback, it is possible to obtain a laser emission from the 6 µm-wide waveguide. Thus, two dielectric mirrors having a 99.9% reflectivity at 1555 nm have been placed on the two waveguide's facets. The pump is injected inside the device using the setup described in Fig. 6-a). The Faby-Perot laser emission spectrum of the w=6 µm waveguide is shown in Fig. 6-b). The low power emitted can be attributed to the low transmission of the output mirror, as well to the feedback losses due to some mirror misalignments.
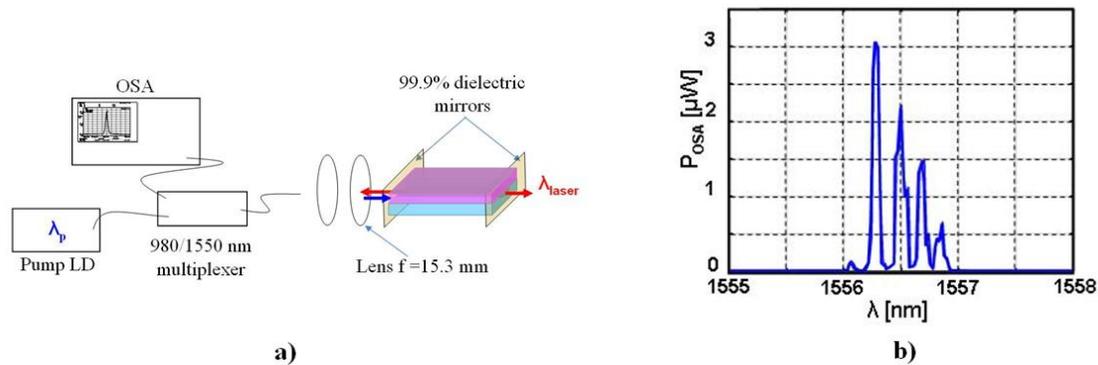

Figure 6: (a) Experimental setup: passing through the multiplexer and a set of lenses, the pump is injected in the waveguide. The emitted laser radiation spectrum is recorded with the OSA connected to the 1550 nm branch of the multiplexer. (b) Measured spectrum for a pump launched power of 339.9 mW.

The Fabry-Perot laser demonstrates that it is possible to realize a hybrid laser using the proposed hybrid structure. We thus describe the procedure to fabricate a single mode hybrid DFB laser operating at λ = 1534 nm.

5.   HYBRID DFB LASER

The new ion-exchange parameters used to obtain the DFB hybrid laser can be found in table 2.

Table 2.Summary of exchange parameters used to make realize the hybrid amplifier.

	GO14	IOG-1
T	330°C	320°C
t_{ex}	3 min	1 min
c_{Ag}	5.2%	7.7%

The 2.5 cm-long Bragg grating has been realized on the passive glass surface with a 4 min-long RIE. The grating has a period of (506.0±0.5) nm and a depth of (12±2) nm. In Fig. 7, we can see an image of an AFM measurement of the patterned GO14 surface.
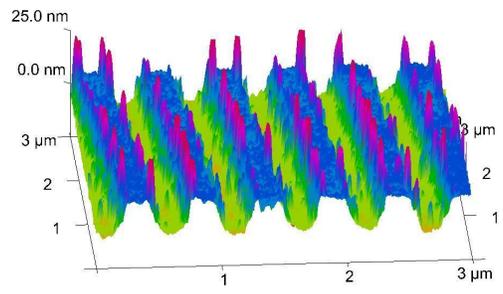

Figure 7: AFM measurement of the Bragg grating patterned on the passive glass substrate

5.1 Device characterization

The near field analysis determined that the waveguide are single-mode at λ =1054 nm for w < 4.5 µm and at 1550 nm for w < 6.5 µm. The optical transmission of the structure around λ_B is characterized by synchronizing the TUNICS tunable laser source and the OSA, as shown in Fig.8-a). A HI1060 fiber is used to inject the signal in the device and a second one to connect the device output to the OSA. The results of this characterization, for a w = 5 µm waveguide, can be seen in Fig.8-b). In this figure we can see that, as expected, the Er^{3+} absorption cross-section is not constant. Moreover, for λ between $\lambda°=°$1533.9 nm and λ = 1534.5 nm, the transmitted power drops of at least 40 dB. This effect assesses the interaction between the guided mode and the Bragg grating. Furthermore, the strong and saturated reflection peak points out that a 12 nm-deep grove is sufficient to obtain a huge reflecting effect mainly because of the strong interaction between the guided mode and the encapsulated grating.
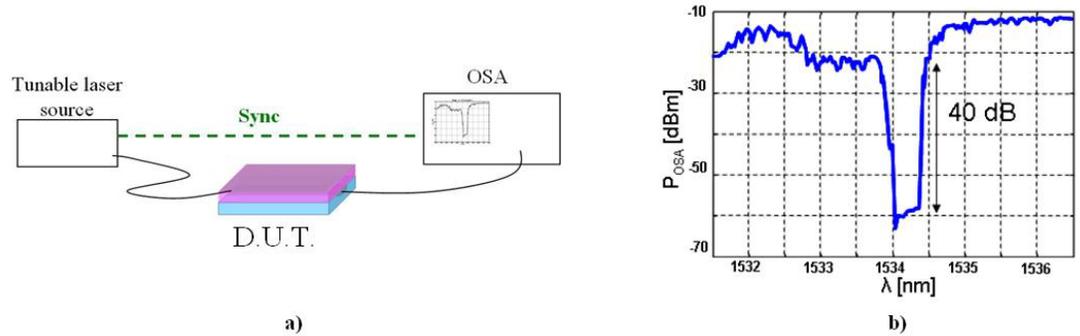

Figure 8: (a) experimental setup (b) device transmission around the Bragg wavelength

Since the Bragg reflection wavelength λ_B has been properly centered around the Er^{3+} peak gain at 1534 nm wavelength, laser operation has been characterized using the setup illustrated in Fig.9. The 1550 nm branch of the multiplexer is used to evaluate the total power and the laser spectrum emitted by the device.
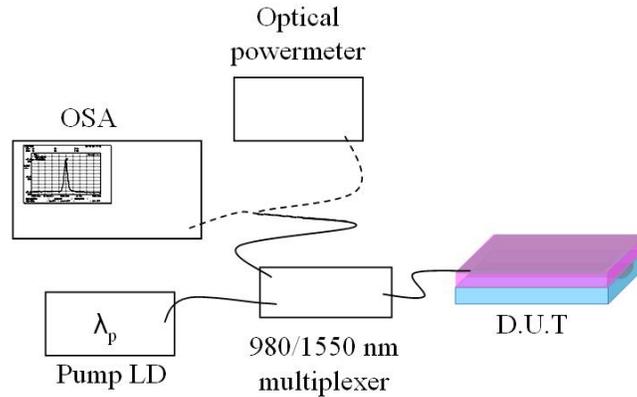
Figure 9: Laser Power and spectrum characterization setup.

Laser effect is observed for waveguides presenting a diffusion aperture width between 3.5µm and 5 µm. As can be seen in Fig.10-a), the highest output power, of (159±5) µW, is attained by the guide having w = 5 µm, with 339.9 mW launched pump. The efficiency of the different waveguides is around 0.09%. The waveguide width w has a strong influence on the threshold and on the maximum emitted power. Further studies are needed to explain this dependency. As expected the laser emission wavelength vary with w, see Fig.10-b). An increase of w leads to an increase of the n_{eff} of the guided mode, and according to the Bragg law (1) to an higher $\lambda_{B.}$. Because of this effect we obtained a DFB hybrid laser matrix component with a ratio between the emitted wavelength over the exchange window of 0.8 nm/µm.
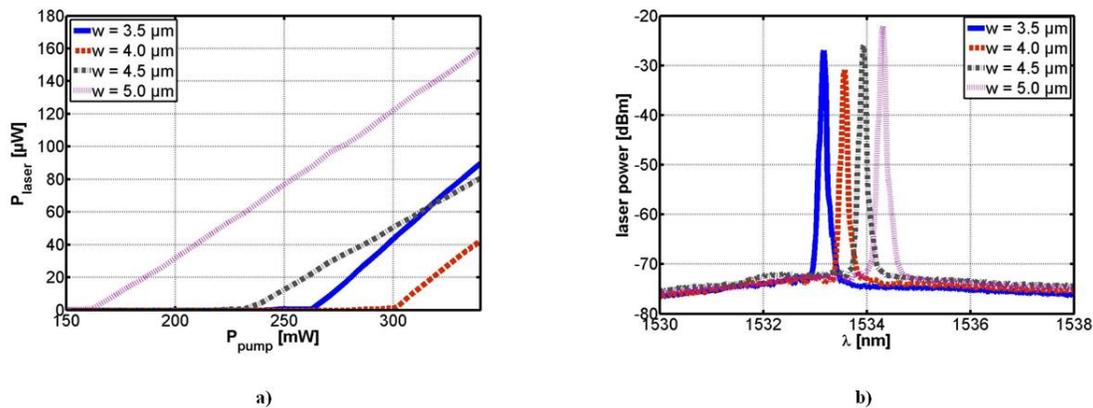

Figure 10: (a) laser power and (b) laser spectrum

6. PESPECTIVES AND CONCLUSION

In this paper we presented an hybrid structure architecture based on Ag^+/Na^+ ion exchange and wafer bonding. Using a GO14 silicate passive substrate and a IOG1 2.2 wt%Er_2O_3 and 3.6 wt% Yb_2O_3 doped glass, we demonstrate the potential of this structure realizing an hybrid amplifier and a hybrid DFB laser. We measured a (1.9±0.9) dB/cm gain coefficient for the hybrid amplifier for a launched pump power of 339.9 mW. Concerning the hybrid DFB laser, for the same pump power, we obtained (159±5) µW emitted power for an ion-exchange window w = 5 µm. Laser emission has been observed for w ranging from 3.5 µm to 5 µm. The size w does not seem to have a huge impact on the laser efficiency: around 0.09% for the different waveguides. On the other and the laser spectrum varies with respect to the exchange window width with a ratio λ/w of 0.8 nm/µm. Theoretical study and device modeling are in progress to improve the laser and amplifier performances. Reliability tests have to be done on the hybrid DFB laser to validate its potential application as a source in telecommunication and LIDAR systems. Moreover we expect to take advantage of this hybrid architecture to fully integrate on the same substrate active and passive functions.

REFERENCES

[1] A. Tervonen, B. R. West and S. Honkanen, "Ion-exchanged glass waveguide technology: a review", Opt. Eng. 50, 071107 (2011)

[2] J.-E. Broquin, "Glass integrated optics: state of the arts and position towards others technologies", Proc. SPIE 6475, 647507 (2007)

[3] L. Bastard, S. Blaize and J.-E. Broquin, "Glass integrated optics ultra narrow linewidth DFB Lasers for DWDM applications", Optical Engineering 42(10), 2800-2804 (2003).

[4] L. Bastard, F. Gardillou, C. Cassagnettes, J.-P. Schlotterbeck, P. Rondeau and J.-E. Broquin, "Development of an ion-exchanged glass integrated optics DFB laser for LIDAR application", Proc. SPIE 7218, 721817 (2009)

[5] F.Gardillou, L. Bastard and J.-E. Broquin, "Integrated optics Bragg filters made by ion exchange and wafer bonding", Appl. Phys. Lett. 89, 101123 (2006)

[6] L. Onestas, D.Bucci, E. Ghibaudo and J.-E. Broquin, "Vertically Integrated Broadband Duplexer for Erbium-Doped Waveguide Amplifiers Made by Ion Exchange on Glass", IEEE Photonics Technology Letters 23(10), 648-650 (2011)

[7] T. Ohtsuki, S. Honkanen, N. Peyghambarian, M. Takahashi, Y. Kawamoto, J. Ingenhoff, A. Tervonen and K. Kadono, "Evanescent field amplification in Nd^{3+} doped fluoride planar waveguide", Appl. Phys. Lett. 69, 2012 (1996)

[8] F. Gardillou, L. Bastard, and J.-E. Broquin, "4.25 dB gain in a hybrid silicate/phosphate glasses optical amplifier made by wafer bonding and ion-exchange techniques",Appl. Phys. Lett. 85, 5176 (2004)

[9] D. L. Veasey, D. S. Funk, P. M. Peters, N. A. Sanford, G. E. Obarski, N. Fontaine, M. Young, A. P. Peskin, W.-C. Liu, S. N. Houde-Walter and J. S. Hayden, "Yb/Er-codoped and Yb-doped waveguide lasers in phosphate glass", Journal of Non-Crystalline Solids, Volumes 263–264, (2000)